OPTIMIZATION OF A LIDAR RECEIVING SYSTEM: ON ESTIMATION OF THE EFFICIENCY OF DIFFERENT RECEIVING OBJECTIVES

A.I. Abramochkin and A.A. Tikhomirov

Institute of Optical Monitoring,
Siberian Branch of the Russian Academy of Sciences, Tomsk
Received April 8, 1998

Different objectives are considered in the paper as candidates for the receiving antennas of a lidar. Those are lenses (three types), mirrors (two types), combination of a mirror and a lens (three types), and multicomponent objectives of two types. The comparison is being done using some generalized quality criteria. The technique proposed for making a comparison together with power and size diagrams allow one to select an optimal objective according to the coefficient of relative efficiency introduced or aiming at minimum length (at the same clear aperture). It is shown that the most compact objectives are those constructed following the Mangene scheme, the Fresnel lenses, and the multicomponent ones (in the order of increasing size).

INTRODUCTION

The optical receiving system, as well as the transmitting one, is one of the main lidar parts, that determines its power potential.[1] Normally, it is composed of a receiving objective, spatial and spectral filters, polarization optical components, and a photodetector. Lenses, mirrors, and mirror-lens objectives are often used as lidar receiving optics. The field stop diaphragm plays the part of spatial filter[2–4] in most lidar receiving systems. If an interference filter is used for spectral selection, a Fabry lens is normally placed in front of it to reduce the angular width of the radiation beam incident on the filter. In Raman lidars[5–7] entrance slit of a monochromator plays the part of a spatial filter, if the monochromator is used as a spectral filter for isolating Raman lines from the spectrum of radiation received from the atmosphere.

Great variety of receiving systems[5,8–10] of different types that exists makes necessary the development of a justified approach to choosing a proper receiving optics when constructing a new lidar. In this paper, we propose some generalized quality criteria for comparative analysis of different objectives and for choosing a proper type for a lidar under the development.

1. FEATURES REQUIRED FROM THE LIDAR RECEIVING OBJECTIVES

When developing a lidar receiving system, telescope objective schemes have been used as the basis. Regardless of the fact that they have many common features, they may have many essential differences. The main difference is that the lidar objective images a scattering volume sounded, that moves along the lidar optical axis, in the subject space, with the speed of light, while in its nominal use a telescope constructs image of an emitting light source that is at infinite distance. As a result, the angles of scattered radiation arrival at the receiving aperture of a lidar objective vary with range at which the sounding pulse is scattered. This, in its turn, makes the image of scattering volume to move in the image space, conjugated with the subject space along and across the optical axis of a telescope.[2,3] That clearly manifests itself in lidars with biaxial optical arrangement when the transmitter and the receiver optical axes do not coincide, especially in the objectives having a long focal length.

The lidar sensing techniques are mostly based on the analysis of power and polarization properties of the backscattered radiation.[5,8–10] Therefore, the main requirement to the lidar receiving objective is to collect and transmit, to a photodetector, as large portion of the backscattered flux as possible. When using multiwavelength lidars, as well as differential absorption and Raman lidars spectral analysis of lidar returns is to be performed along with power measurements. In this case, it is necessary to take into account chromatic aberrations of the objective used. Finally, in lidars for investigation of atmospheric turbulence,[11] the main task to be achieved is to accurately image the scattering volume.

By the type of platform used to deploy a lidar, one can distinguish between the stationary and mobile lidars. As to the former ones there are practically no any limitations on their mass and size, so they use receiving objectives of large diameters and, correspondingly, heavy ones.[12,13] The mobile lidars,

0235-6880/98/08 768-08 $02.00 © 1998 Institute of Atmospheric Optics

both ground-based and especially spaceborne ones,[16,17] have certain mass and size limitations. The classification of the receiving objectives by size that we propose here is given in Table I.

TABLE I. Size of lidar objectives.

Type of a lidar	Objective size	Objective diameter, m
Stationary	Very large	≥ 1.0
	Large	0.5–1.0
	Medium-sized	0.3–0.5
Mobile	Large	0.3–0.5
	Medium-sized	0.2–0.3
	Small	≤ 0.2

2. PARAMETERS CHARACTERIZING THE RECEIVING OBJECTIVE

Any receiving objective of a lidar is characterized by two main parameters that enter, as the instrumental constants, into the lidar equation. These are the effective receiving area S_{ef} and the transmittance K. In general, we can estimate quality and efficiency of an objective using a number of characteristics. Among those we would separate out, according to Ref. 18, the following ones: 1) size and mass; 2) power; 3) aberration; 4) spectral; 5) technical and economical; 6) performance characteristics.

Size and mass characteristics determine the length and the cross size of an objective and its components, their mass and mutual position, as well as the location and size of a scattering volume image. Most important characteristics of those are: the diameter D_o, the focal length f, and ratio $A = D_p/f$, where D_p is diameter of the input pupil. The terms "clear apertureB or "input aperture diameter" that are used in lidar engineering are equivalent to D_p value. The diameter D_o exceeds D_p by the mount housing thickness.

The focal length f determines the size of the scattering volume image[2,3] in the plane where spatial filter is set as well as the longitudinal size L of the objective. The values f, D_p, and B (the distance between optical axes of the transmitter and the receiving objective) enter into the relations that determine the lidar overlap function and the dynamic range of the received signal.[2,4,5]

The mass of the objective and its components depends on materials used for refracting and reflecting elements, metal mounts and tubes, as well as the rigidity demanded. Since, based on rigidity calculations, the thickness of mirrors and lenses is chosen in terms of fractions of their diameter, $t = (0.08 - 0.15)D_o$ (Refs. 19 and 22), the mass of the objective optical elements may be considered, in the first approximation, proportional to the third power of diameter, i.e., $m_o \sim D_o^3$.

Power characteristics determine parameters of the receiving objective as a converter of the backscattered radiation. Among these parameters there are: light-collecting power (squared F/D ratio of the input pupil), which is proportional to its area, and its transmittance. The latter accounts for losses associated with reflection from mirror surfaces, radiation scattering and absorption in the lenses and meniscus elements. Flux screening by the elements located in front of the primary mirror is accounted for by introducing the effective area S_{ef} of the receiving objective.

The power of radiation scattered on the components of the receiving objective,[23] that decreases the signal-to-noise ratio as well as the field-of-view angle Ω influencing the value of this ratio in the presence of background radiation,[5] should also be considered among the power characteristics. However, it would be more correct to consider the parameter Ω as the characteristic of the receiving system as a whole. Usually, the value of the plane field-of-view angle θ does not exceed 3 mrad, except in the lidars for investigation of multiple scattering, where it may be more than 10 mrad. The field of view size and shape optimization is one of the essential steps to increasing the signal-to-noise ratio at the output of the lidar receiving system.[2–5]

Aberration characteristics enable one to estimate the quality of an image constructed with an objective and depend on dimensions, the radius of curvature of the reflecting or refracting surfaces, thickness and the refractive index of an optical material. Lidar receiving objectives have, as the telescopes, monochromatic or chromatic aberrations.[19–21] The former ones are independent of the incident radiation wavelength; they appear due to different conditions of refraction or reflection for different parts of the flux. Among those there are spherical aberration, coma, astigmatism, field aberration, and distortion. The chromatic aberrations are caused by dispersion of multiwavelength radiation in the optical elements.

Spherical aberration is most essential for the receiving objectives of single-frequency lidars with $\theta \le 3$ mrad. The diameter of the least aberration circle characterizes this aberration most comprehensively. This diameter is described by the relation

$$\delta_{sph} = k\, f\, A^3, \qquad (1)$$

where k is the coefficient, which depends on the receiving objective type ($k = 0.0156$ for a spherical mirror and $k \approx 0.137$ for a plane-convex lens[19,22]).

Spectral characteristics are determined by the lidar operating wavelength range $\lambda_1 - \lambda_n$ or by its single wavelength λ_0. These characteristics impose restrictions on the lens material or the material of mirror coating. The influence of chromatic aberrations is significant for the spectrometric lidars. As a result simple lens objectives cannot be used in such lidars, unless the lens chromatism is specially used for wavelength selection in a focal monochromator.[24]

Technical, economical, and performance characteristics allow one to estimate the quality, reliability, and economic feasibility of the objective design, as well as its operation efficiency.

When calculating such characteristics of a lidar as sounding range, the accuracy of determining the atmospheric parameter sought, etc., we can find dimensions, power and aberration characteristics. The technical and economical characteristics are defined on the basis of specific technical approach, i.e. the manufacturing of the objective with certain overall dimensions, power and aberration characteristics. The objective cost depends on both its diameter and optical surface profile (sphere, parabola, etc), that is determined by the technology of production. The performance characteristics show the complexity of the adjustment process, as well as testing quality and technical state of an objective during its operation.

3. TYPES OF LIDAR RECEIVING OBJECTIVES

According to classification given in Ref. 19, the objectives may be classified into three groups: lens, mirror, and lens-mirror ones. All three types are used in lidar receiving systems. The main schemes are presented in Table II together with some limiting parameters. There are certain technological limitations that determine maximum diameter of a mirror objective in accordance with the Table I.

Lens objectives. An objective based on the single lens with spherical surfaces is the simplest one for single-wavelength lidars. The spherical aberration of such an objective can be reduced by optimal choice of the radii of curvature of the refracting faces. However, the parameter A in this case is limited by the values of $1/4 - 1/6$, what increases the objective length. Increasing A up to $1/2$ is undesirable, because it leads to an enhanced size of the least aberration circle (see Eq. (1)). As this takes place one should correspondingly increased field-of-view angle of the receiving system to avoid vignetting. This, in turn, leads to a decrease in the signal-to-noise ratio when operating under conditions of background illumination.

The single-lens objective having an aspherical input and a plane outputs surface could be most optimal in this case. Such an objective may have the D/F ratio equal to $1/2$ with the angular size of the least aberration circle due to spherical aberration no more than 0.66 mrad. It is already not so bad for a lidar receiver. Such objectives are widely used in the modern models of mobile lidars.[16]

TABLE II. Comparative characteristics of the lidar receiving objectives.

Type	Appearance, optical scheme	Parameters
Lens	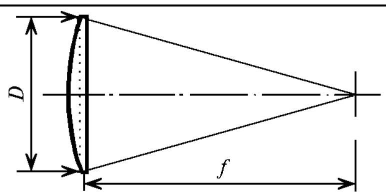	Spherical (aspherical) lens $A_{max} = 1/4$ (1/2); $D_{max} = 400$ mm; $S_{ef} = \pi D^2/4$; $K_{max} = 0.96$; $\overline{K\,S_{ef}} = 0.96$; $m_o \sim D^3$; $L \approx f$; $L_{min} \approx 4.12\ D$ (2.12 D for aspherical lens)
	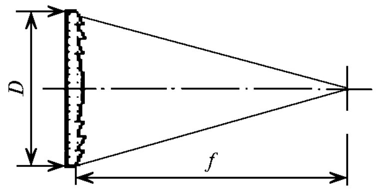	Fresnel lens $A_{max} = 2.0$; D_{max}; = 500 mm $S_{ef} = \pi D^2/4$; $K_{max} = 0.9$; $\overline{K\,S_{ef}} = 0.90$; $m_o \sim D^3$; $L \approx f$; $L_{min} \approx 0.5\ D$
Mirror	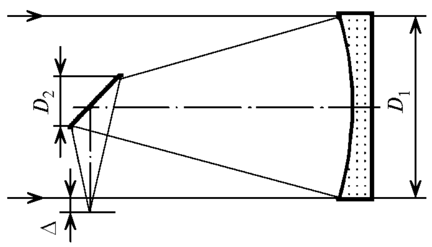	Newtonian reflector $A_{max} = 1/4$ (1/2); D_{max} is unlimited; $S_{ef} = \pi D_1^2 (1 - q^2)/4$; $K_{max} = 0.8$; $q_{max} = 0.125$; $\overline{K\,S_{ef}} = 0.787$; $m_o \sim D_1^3 (1 + q^3)$; $L \approx f_1 (1 - q) + D_2/2$; $L_{min} \approx 3.67\ D_1$
	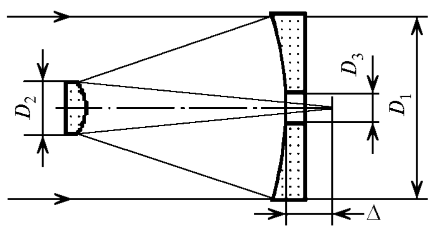	Cassegrainian objective $A_{max} = 1/8$; D_{max} is unlimited; $S_{ef} = \pi D_1^2 (1 - q^2)/4$; $K_{max} = 0.8$; $q_{max} = 0.3$; $\overline{K\,S_{ef}} = 0.728$; $m_o \sim D_1^3 (1 + 2.8\ q^3)$; $L \approx f_1\ q/\beta$; $L_{min} \approx 2.44\ D_1$

Table II continued

	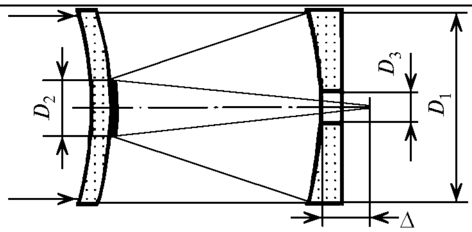	Maksutov objective $A_{max} = 1/6$; D_{max} is unlimited; $S_{ef} = \pi D_1^2 (1 - q^2)/4$; $K_{max} = 0.75$; $q_{max} = 0.3$; $\overline{K S_{ef}} = 0.682$; $m_o \sim 2 D_1^3$; $L \approx f_1 q/\beta$; $L_{min} \approx 2 D_1$
Mirror-lens	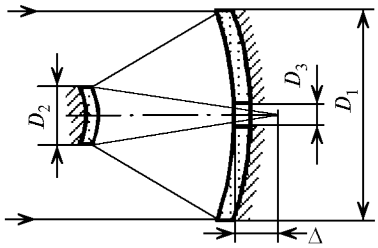	Mangene objective $S_{ef} = \pi D_1^2 (1 - q^2)/4$; $K_{max} = 0.72$; $q_{max} = 0.3$; $\overline{K S_{ef}} = 0.655$; $m_o \sim D_1^3 (1 + q^3)$; $L \approx f_1 q/\beta$; $L_{min} \approx 0.31 D_1$
	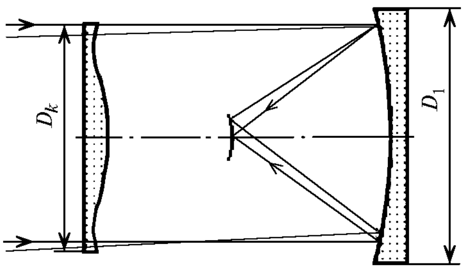	Schmidt objective $A_{max} = 1/2$; D_{max} is unlimited; $S_{ef} = \pi D_k^2/4$; $K_{max} = 0.85$; $q_{max} = 0.15$; $\overline{K S_{ef}} = 0.850$; $m_o \sim 2 D_1^3$; $L \approx 2 f$; $L_{min} \approx 4.2 D_1$
Multicomponent lens	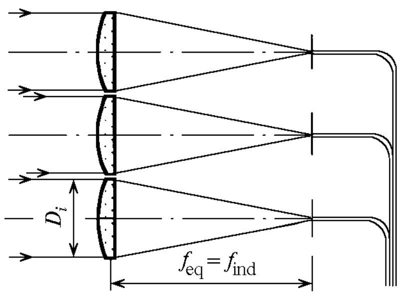	Aspherical lenses $f_{eq} = f_{ind}$; $A_{ind\ max} = 1/2.5$; $A_{eq} = \sqrt{n} A_{ind}$; $S_{ef} = n S_{ef\ ind}$; $K_{max} = 0.96$; $L \approx f_{ind}$; $L_{min} \approx 2.62 D_{ind}$; $L_{min} \approx 0.99 D_{eq}$ (for 7 lenses) $\overline{K S_{ef}} = 0.794$
Multicomponent mirror	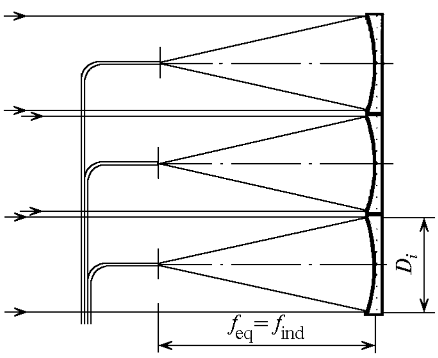	Parabolic mirrors $f_{eq} = f_{ind}$; $A_{ind\ max} = 1/2.5$; $A_{eq} = \sqrt{n} A_{ind}$; $S_{ef} = n S_{ef\ ind}$; $K_{max} = 0.9$; $q_{min} = 0.05$; $L \approx f_{ind}$; $L_{min} \approx 2.62 D_{ind}$; $L_{min} \approx 0.99 D_{eq}$ (for 7 mirrors) $\overline{K S_{ef}} = 0.744$

The advantages of the glass lens objective are: ease in use, high transmittance, K equal to 0.92 or even 0.96 if antireflection coated for use in single-frequency lidars. It also provide for low level of scattered radiation. Usually D_o = 300–400 mm that is caused by the production process of high-quality optical workpiece and lenses.

The objectives based on Fresnel lenses were also used in lidars.[25] These lenses are easy for manufacturing and may have significantly less spherical aberration as compared to the usual spherical lenses.[21] The Fresnel lens made of organic glass has the thickness t and the mass m_o several times lower than spherical or aspherical lenses made of glass or quartz with the same diameter

D_o. Therewith the value of A is no more than two.[26] However, the Fresnel lenses have some serious drawbacks. It is high level of parasitic light scattering on the zone borders, that leads to a decrease in the signal-to-noise ratio. There is also some screening of slant beams by the ring cylindrical surfaces. Because of these drawbacks Fresnel lenses are used in the lidar receiving systems only in some special cases.

The multicomponent objectives having two or three lenses are useful only in multiwavelength lidars for correction of chromatic aberrations. However, their use leads to a bigger size and higher costs, and gives no advantages as compared to the mirror objectives.

Mirror objectives. Use of such objectives allows one to decrease the longitudinal size as compared to the lens one of the same diameter D_p. Besides, the metal coating provides for operation in a wide spectral range that is important for multiwavelength lidars. These objectives are widely used in both stationary[12,13] and mobile lidars.[14–17] Since the mirror focal surface is on the same side, from where a radiation flux comes, a part of radiation is screened by a photodetector or a secondary mirror. The photodetector is placed at the focus only in lidars with a large mirror diameter.[13] Double-mirror objectives are used more often. In such objectives, the primary mirror has the diameter D_1 and the focal length f_1, and the secondary mirror has the parameters D_2 and f_2. Such an objective is characterized by an equivalent focal length f_{eq}, which is usually longer than f_1, and smaller ratio $A_{eq} = D_1/f_{eq}$. The secondary mirror reduces the effective objective area S_{ef}, what is accounted for by the screening factor $q = D_2/D_1$. The value of q is usually chosen to be below 0.3, therewith the effective area S_{ef} reduces by less than 10%. The parameter β is also introduced, which characterizes change in the beam convergence after the secondary mirror, i.e. change of the D/F ratio,

$$\beta = A_{eq}/A_1 = f_1/f_{eq}. \quad (2)$$

The ratio $f_1/f_2 = (1 - \beta)/q$ relates the focal lengths of the primary mirror and the secondary one. Calculations of dimensions of a double-mirror objective are considered in detail in Ref. 19. The distance between mirror apices is

$$d = (1 - q)\, f_1, \quad (3)$$

the length of the focal plane overhang from the primary mirror apex is

$$\Delta = [q - \beta\, (1 - q)]\, f_{eq} \quad (4)$$

(except for Newtonian objectives). In the first approximation (neglecting the secondary mirror thickness), the longitudinal dimension of the mirror objective is

$$L \approx f_{eq}\, q = f_1\, q/\beta. \quad (5)$$

The maximum value of the transmittance K for two aluminum-coated mirrors equals 0.8 within the spectral interval 0.2–1.0 μm (Ref. 19). The central through aperture of the diameter

$$D_3 = \Delta A_{eq} - 2d\, [(f_{eq} + \Delta) \tan \theta/2]/(d - \Delta) \quad (6)$$

in the primary mirror provides for a free passage of all beams arriving within the angle θ to the focal plane without any vignetting.

The Newtonian objective has the diagonal plane mirror as the secondary mirror, so in this case $f_{eq} = f_1$. To minimize the value of q, the focal plane is carried out at a minimum distance Δ_N beyond the diameter D_1. The value Δ_N is defined in dimension calculations as[19]:

$$\Delta_N = [(f_1 - D_1/2) \tan \theta/2]\, (1 + \tan \theta/2). \quad (7)$$

The value of q factor should not exceed 0.125. This particular objective has an essential disadvantage, that is its transverse dimension increases at increasing L value. For that reason it was used only in the early constructed lidars,[14,27,28] in particular, in coaxial transceiving systems. The presence of a diagonal mirror does not allow the use of these objectives in the polarization lidars.

The Cassegrainian-type objectives are mostly used in mobile lidars. It normally consists of a parabolic primary mirror and a hyperbolic secondary one. The focal plane overhang Δ beyond the primary mirror apex enables one to mount spatial and spectral filters, the polarization elements, and the photodetector behind the primary mirror. The Cassegrainian optical arrangement provides for A_{eq} ratios no more than 1/8. In this case, the telescope length is much less than its equivalent focal length, and the angles of incidence onto each mirror are small. It practically does not change the incident radiation polarization. All this favors the use of such receiving objectives in polarization lidars as well. Use of only two reflecting surfaces provides for high K values.

We do not consider here the Gregorian scheme, because its secondary mirror is placed behind the focal plane, that makes its length L essentially longer as compared to the Cassegrainian scheme.

Mirror-lens objectives. The Maksutov objective (meniscus Cassegrainian) is most widespread. The objective consists of the meniscus lens compensator and the primary mirror. All surfaces are spherical that is the significant advantage for the objective production technique. To simplify the design, the secondary mirror is sometimes coated onto the central part of meniscus. With use of an achromatic meniscus,[19] it is possible to make the objective operating within the wide spectral range. Besides, the meniscus executes, at the same time, the protection function that improves its operation characteristics. This objective is preferable for the mobile lidars.[15]

The combination of the mirror and lens components gives greater light-gathering power at a better correction for aberrations as compared to mirror objectives. The meniscus diameter in the Maksutov scheme is equal to the primary mirror diameter, what increases the objective cost. P.P. Argunov has suggested the aplanat system, which has a corrector instead of the secondary mirror. This corrector is composed of achromatic lens doublet having a mirror coating on the rear surface.[19,29] In this case all optical components surfaces are spherical. Such a system, at $A_{eq} = 1/3.3$, simultaneously corrects spherical aberration, coma, as well as chromatism for two wavelengths (this objective is not presented in Table II).

When using the Mangene scheme, the reflecting coating is coated onto the rear side of every optical element that allows use of its refractive properties. The mirror lens may be steadily achromatic with corrected spherical aberration.[30] The main advantage of such an objective is small system size, as well as the possibility to get small residual aberrations at large relative apertures. The A_{eq} value may reach unity or even more.[30] Silver mirror coatings coated onto the lens rear side may be protected against the atmospheric influences by films. The silver coating increases the reflection coefficient by 7% as compared to aluminum one. The disadvantages of this objective are the following: process difficulties when manufacturing, sensitivity to deformation and center displacement. The Mangene objective has been used in the Russian space lidar.[17]

The Schmidt camera. The correcting plate placed in the input mask plane, that coincides with the curvature center of the spherical mirror, excludes a number of aberrations.[19] Its central part acts as a weak positive lens, which shortens the focal distance for both paraxial and inside-zone beams. The middle part is neutral, while the outer part acts as a weak negative lens. This results in focus displacement for all beams toward the mirror apex. The Schmidt camera is free of spherical aberrations, coma, astigmatism, and third-order distortion. Chromatism, residual coma, and astigmatism caused by correction plate presence are rather small.[19] To obtain a linear field with the diameter $2a$ without vignetting, the mirror diameter should exceed the correction plate diameter by $4a$, i.e. $D_1 = D_{cor} + 4a$. The central screening of beams passing through the correction plate is $q = 2a/D_{cor}$. The merit of the Schmidt camera is the feasibility to obtain a large field-of-view angle, up to 6–7°. Using the Schmidt camera, we have developed the wide-angle receiving objective for the meteorological lidar, which measures the wind velocity by the correlation method.[8] A spatial filter construction used gave an opportunity to use one photodetector for recording the return signals from three different directions in the narrow instant fields of view, when the total field of view was large. This has eliminated the necessity to rotate the massive objective having the diameter $D_1 = 400$ mm.

Multicomponent compound mirror and lens systems. The enlargement of the receiving objective diameter necessary for increasing the lidar power potential leads to growth of its weight and cost. Therefore, in recent years the spatial synthesis of the receiving apertures in the compound objective is used. Such an objective consists of the nearby small-size lenses or mirrors.[32,33] It allows significant decrease in the weight and the longitudinal size of the receiving system. Such an objective has been realized in the Raman lidar.[6]

It can be derived geometrically that the compound objective consisting of seven round small objectives closely packed has the maximum ratio of the areas $\Sigma S_i / S_{bc} = 0.778$, where S_{bc} is the area of the big circle including small objectives. Provided that small objectives are hexagons, this ratio equals 0.827. We do not consider here synthesized adaptive systems that solve the problem of phase matching of fluxes transformed by every element.

A light-guide fiber end is set at the focus of each mirror (lens). The radiation flux received is transported to the spectral filter or photodetector through this fiber. The relative aperture of each element of the compound objective is limited by the numerical aperture ($A_f \le 1/2$) of the fiber used.[34] Application of light guides makes simpler matching of the output objective aperture and the spectral device entrance slit, that is the urgent problem in the Raman lidars.[6,7] In this case, the input end of the multi-fiber light guide acts as a spatial filter. The presence of several elementary "objective – light-guide" systems in the receiver and the possibility to group correspondingly light-guide output ends allow performance of the spatial transformation of the received radiation, that is impossible to do by any other methods. The another advantage is increase of S_{ef} and A_{eq}, because in this case an equivalent focal distance f_{eq} keeps equal to focal distance f_i of elementary objective, but the effective diameter $D_{ef} \approx \sqrt{n}\, D_i$ (at the great number of objectives). The main demerits of the multi-component compound objective are cumbersome adjustment of optical axes of different objectives, as well as additional signal losses when inputting radiation into the light guide and inside the light guide.

4. CRITERIA OF EFFICIENCY ESTIMATION AND COMPARISON OF RECEIVING OBJECTIVES

From the efficiency viewpoint, it is expedient to compare the objectives. The comparison may be done in KS_{ef} value achieved, all other factors being the same; as well as in size and mass characteristics, the cost of objective production at the same KS_{ef} values. The main parameters of the above-considered objectives are: the maximum relative aperture A_{max}; the effective area S_{ef}; the maximum transmittance K_{max}; the screening factor q_{max}; the relative efficiency coefficient $\overline{K\,S_{ef}}$; the objective mass m_o (without metal details); the objective minimum length L_{min}. All these parameters are given in Table II.

The $\overline{K S_{ef}}$ value is the product of K_{max} by S_{ef} scaled to the square of an ideal objective of the same diameter with $K_{max} = 1$ and $q = 0$. For the lens objective $L_{min} = f + t \approx D_p(1/A_{max} + 0.12)$. For mirror objective (except the Newtonian one) and mirror-lens (except the Maksutov scheme) $L_{min} = f_{eq}q + tq = qD_p(1/A_{max} + 0.12)$. For the Maksutov scheme, it is necessary to take into account the longitudinal size of a meniscus with the diameter D_p.

Figure 1 presents the efficiency diagram for the objectives considered above. The maximum achievable values of the relative efficiency $\overline{K S_{ef}}$ for different objectives (at the same clear apertures D_p) are laid off as ordinate, the minimum possible longitudinal dimension L_{min} expressed in terms of diameter is laid off as abscissa. In view of the fact that the D_p values for all objectives are taken the same in the diagram, it is possible, in the first approximation, to believe that the volume and, consequently, the mass of an objective (with the metal frame) are proportional to the length L_{min}. The objectives presented in the diagram are divided into three groups: 1) very compact, $L_{min} \le D_p$ (the Mangene scheme, the Fresnel lens, a compound objective); 2) compact, $L_{min} = (2 - 3)D_p$ (the Maksutov and Cassegrainian schemes, aspheric lens); 3) large-size $L_{min} \ge 3.5D_p$ (the Newtonian scheme, a spherical lens, the Schmidt camera).

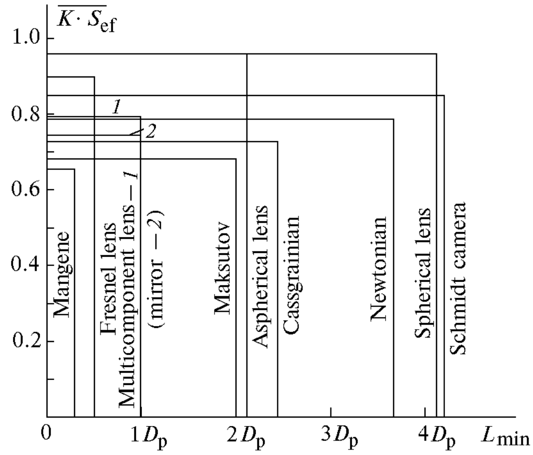

FIG. 1. Diagram of power and size characteristics for different types of the receiving objectives.

The diagram and numerical values of the limit parameters presented in Table II and in the figure allow us to determine, for example, that D_p for the Mangene objective should be increased by a factor of $\sqrt{(\overline{K S_{ef}})_{lens}/(\overline{K S_{ef}})_{Mang}} \approx 1.21$ in order to get the same coefficient of the relative efficiency as the antireflection lens objective. So, in the limit case, the antireflection lens objective with the diameter $D_p = 200$ mm is equivalent in $\overline{K S_{ef}}$ value to the Mangene objective with $D_p = 242$ mm. At the same time, L_{min} of the Mangene objective also increases by a factor of 1.21, i.e. it enlarges from 62 to 75 mm, but it won't achieve $L_{min} = 100$ mm for the Fresnel lens with the diameter $D_p = 200$ mm. If, for example, the diameter of the aspheric antireflection lens objective is decreased by a factor of 1.21, in order to equalize it in $\overline{K S_{ef}}$ value with the Mangene objective, i.e., to make it equal to 165 mm, then its L_{min} will reduce from 424 to 350 mm. So L_{min} becomes less than that for the Maksutov objective with $D_p = 200$ mm ($L_{min} = 400$ mm). Following the technique suggested, similar comparisons could be done for other objectives.

When comparing the objective efficiency, one should take into account that objective cost grows as, at least, D_o^2 or even as $D_o^{2.7}$ (see Ref. 35). At the same time, it should be noted that the production cost depends on materials used, reflecting and refracting surface profiles, production process, and production possibilities. Therefore, the cost hardly can be compared analytically. Nevertheless, by the relative production cost, the objectives can be ordered as follows (in the cost increasing order at the same $D_p \approx 200$–300 mm): the Newtonian scheme, a compound mirror, a spherical lens, the Fresnel lens, a compound aspheric lens, an aspheric lens, the Maksutov scheme, the Cassegrainian scheme, the Mangene scheme, and the Schmidt camera.

CONCLUSION

Generalized criteria for estimation of the quality of the lidar receiving objectives have been suggested. Comparative analysis of the objectives has been made and limit objective parameters have been determined. The objectives have been divided into three groups based on compactness: 1) $L_{min} \le D_p$; 2) $L_{min} = (2$–$3)D_p$; and, 3) $L_{min} \ge 3.5D_p$. The presented technique and the diagram of power and size parameters allow comparison of different types of the objectives when designing lidar transceiving systems.

REFERENCES

1. B.V. Kaul', Atm. Opt. **2**, No. 2, 166–169 (1989).
2. A.I. Abramochkin, S.A. Danichkin, and A.A. Tikhomirov, in: *Abstracts of Reports at the V All-Union Symposium on Laser Sensing*, Institute of Atmospheric Optics SB AS SSSR, Tomsk (1978), Part II, pp. 60–62.
3. S.A. Danichkin and I.V. Samokhvalov, Opt. Mekh. Promst., No. 5, 5–8 (1979).
4. A.A. Tikhomirov, in: *Measurement of the Atmosphere Optical and Meteorological Parameters Using Laser Radiation* (Publishing House of the

Institute of Atmospheric Optics SB AS SSSR, Tomsk, 1980), pp. 106–114.
5. M.V. Kabanov, ed., *Laser Sensing of Industrial Aerosols* (Nauka, Novosibirsk, 1986), 186 pp.
6. Yu.F. Arshinov and S.M. Bobrovnikov, in: *Regional Monitoring of the Atmosphere*, Vol. 2. *New Devices and Measurement Techniques* (Publishing House of the Institute of Atmospheric Optics SB RAS, Tomsk, 1997), pp. 112–130.
7. Yu.F. Arshinov, S.M. Bobrovnikov, S.A. Danichkin, et al., *Problems of Remote Sensing of the Atmosphere* (Publishing House of the Institute of Atmospheric Optics SB AS SSSR, Tomsk, 1975), pp. 150–153.
8. V.E. Zuev, ed., *Laser Sensing of the Troposphere and the Underlying Surface* (Nauka, Novosibirsk, 1987), 262 pp.
9. R.M. Measures, *Laser Remote Sensing* (John Wiley and Sons, New York, 1987), 550 pp.
10. V.E. Zuev and V.V. Zuev, *Modern Problems of Atmospheric Optics*. Vol. 8. *Remote Optical Sensing of the Atmosphere* (Gidrometeoizdat, St. Petersburg, 1992), 232 pp.
11. V.E. Zuev, V.A. Banakh, and V.V. Pokasov, *Modern Problems of Atmospheric Optics*. Vol. 5. *Optics of the Turbulent Atmosphere* (Gidrometeoizdat, Leningrad, 1988), 270 pp.
12. A.I. Borodavko, N.P. Vorobey, V.I. Gubsky, et al., Opt. Atm. **1**, No. 3, 109–155 (1988).
13. B.V. Kaul', Atmos. Oceanic Opt. **5**, No. 4, 277–281 (1992).
14. R.J. Allen and W.E. Evans, Rev. Sci. Instrum. **43**, No. 10, 1422–1232 (1972).
15. Yu.S. Balin and A.A. Tikhomirov, in: *Regional Monitoring of the Atmosphere*, Vol. 2. *New Devices and Measurement Techniques* (Publishing House of the Institute of Atmospheric Optics SB RAS, Tomsk, 1997), pp. 16–34.
16. A.A. Tikhomirov and V.S. Shamanaev, in: *Regional Monitorimg of the Atmosphere*, Vol. 2. *New Devices and Measurement Techniques* (Publishing House of the Institute of Atmospheric Optics SB RAS, Tomsk, 1997), pp. 58–78.
17. V.E. Zuev, Yu.A. Balin, and A.A. Tikhomirov, Kosmichna Nauka i Tekhnologiya **3**, Nos. 1–2, 16–25 (1997).
18. A.V. Pavlov, *Optical and Electronic Devices (Grounds for Theory and Calculation)* (Energiya, Moscow, 1974), 360 pp.
19. N.N. Mikhel'son, *Optical Telescopes. Theory and Design* (Nauka, Moscow, 1976), 510 pp.
20. M.I. Apenko and A.S. Dubovik, *Applied Optics* (Nauka, Moscow, 1971), 392 pp.
21. M.M. Rusinov, ed., *Computational Optics*. Handbook (Mashinostroenie, Moscow, 1984), 423 pp.
22. R. Hudson, *Infrared Systems* [Russian translation] (Mir, Moscow, 1972), 534 pp.
23. I.V. Dyachenko and N.S. Zakharov, Atmos. Oceanic Opt. **6**, No. 11, 836–839 (1993).
24. A.N. Zaidel', G.V. Ostrovskaya, and Yu.I. Ostrovskii, *Spectroscopy Instrumentation and Practice* (Nauka, Moscow, 1972), 375 pp.
25. H. Shimizu, T. Kobayasi, and T. Inaba, in: *Abstracts of Reports at the 6th Inter. Laser Radar Conf.*, Sendai (1974), pp. 25–26.
26. V.G. Karpov, A.A. Kuprin, and S.N. Natarovsky, *Calculation of Fresnel Optical Systems and Optical Elements* (LITMO, Leningrad, 1986), 54 pp.
27. R.T.H. Collis, Microwaves, No. 3, 94–100 (1969).
28. A.I. Abramochkin, Yu.S. Balin, P.P. Vaulin, et al., in: *Measuring Devices for Investigation of the Near-Ground Atmospheric Layers* (Publishing House of the Institute of Atmospheric Optics SB AS SSSR, Tomsk, 1977), pp. 5–16.
29. P.P. Argunov, Opt. Mekh. Promst., No. 6, 15–20 (1965).
30. D.V. Gavrilov, Opt. Mekh. Promst., No. 6, 55–68 (1967).
31. G.G. Matvienko, Yu.F. Arshinov, A.I. Grishin, et al., in: *Proceedings of the 11th Symposium on Laser and Acoustic Sounding of the Atmosphere* (Institute of Atmospheric Optics, Tomsk, 1993), pp. 130–136.
32. Yu.E. Kuzilin, V.N. Sintsov, and N.A. Sitnik, in: *Proceedings of the All-Union Scientific and Practical Conference on Modern Applied Optics and Optical Devices* (LITMO, Leningrad, 1975), Part 1, pp. 3–6.
33. J. Berbige and A. Huit, eds., *Modern Telescopes* [Russian translation] (Mir, Moscow, 1984), 312 pp.
34. L.M. Kuchikyan, *Light Guides* (Energiya, Moscow, 1973), 176 pp.
35. S.B. Gascoigne, J. Physics, Ser. E **E3**, No. 3, 165–172 (1970).